Title

THE INFLUENCE OF FLUCTUATIONS ON THE CORRELATION BETWEEN EXIT-CHANNEL KINETIC ENERGY AND ENTRANCE-CHANNEL ANGULAR MOMENTUM FOR HEAVY ION COLLISIONS

Authors

Moretto, L.G.
Sobotka, L.G.

Publication Date

1981-07-01

LBL-13007
Preprint

Lawrence Berkeley Laboratory
UNIVERSITY OF CALIFORNIA

Submitted to Zeitschrift für Physik

THE INFLUENCE OF FLUCTUATIONS ON THE CORRELATION BETWEEN EXIT-CHANNEL KINETIC ENERGY AND ENTRANCE-CHANNEL ANGULAR MOMENTUM FOR HEAVY ION COLLISIONS

L.G. Moretto and L.G. Sobotka

July 1981

NUCLEAR SCIENCE DIVISION

Prepared for the U.S. Department of Energy under Contract W-7405-ENG-48

THE INFLUENCE OF FLUCTUATIONS ON THE CORRELATION BETWEEN EXIT-CHANNEL KINETIC ENERGY AND ENTRANCE-CHANNEL ANGULAR MOMENTUM FOR HEAVY ION COLLISIONS

L.G. Moretto and L.G. Sobotka

Nuclear Science Division
Lawrence Berkeley Laboratory
University of California
Berkeley, CA 94720

ABSTRACT

The role of fluctuations on the relationship between the exit-channel kinetic energy and the entrance-channel angular momentum in deep inelastic heavy ion reactions has been studied in the equilibrium limit. Two sources of fluctuations are considered: first, the coupling of the orbital motion to thermally excited angular-momentum-bearing modes, and second, the effect of random shape fluctuations at scission.

This work was supported by the Director, Office of Energy Research, Division of Nuclear Physics of the Office of High Energy and Nuclear Physics and by the Nuclear Sciences of the Basic Energy Sciences Program of the U.S. Department of Energy under Contract W-7405-ENG-48.

1. INTRODUCTION

The large range of ℓ-waves involved in deeply inelastic collisions between heavy ions makes it difficult to experimentally single-out well-defined windows in the entrance-channel angular momentum. Since the exit-channel kinetic energy has been a useful tool for differentiating elastic, quasi-elastic, and deeply inelastic mechanisms and their associated ℓ-wave regions, one might hope that this exit-channel observable could be used to further subdivide the deep-inelastic region. In fact, most theoretical treatments [1-4] indicate that a correlation between exit-channel kinetic energy and entrance-channel angular momentum persists into the deep-inelastic region. However, fluctuations tend to spoil this relationship.

In this paper we shall discuss two sources of fluctuations relevant to this problem: a) the coupling of orbital motion to a thermally excited wriggling mode [5] and b) the effect of random shape fluctuations at scission [6-8].

2. COUPLING OF THE ORBITAL MOTION TO ONE WRIGGLING MODE

Let us consider the simple analytical case of two equal touching spheres with one wriggling mode [5] coupled to the orbital motion.

The exit channel kinetic energy above the Coulomb barrier is:

$$E = \frac{\ell^2}{2\mu d^2} \qquad (1)$$

where ℓ is the exit-channel orbital angular momentum, μ is the reduced mass, and d is the distance between centers, equal to the sum of the radii.

The total rotational energy can be expressed as:

$$E_R = \frac{\ell^2}{2\mathcal{J}^*} + \frac{I^2}{4\mathcal{J}} - \frac{I\ell}{2\mathcal{J}} \tag{2}$$

where I is the entrance channel angular momentum, $\mathcal{J}$ is the moment of inertia of one of the two spheres, and $\mathcal{J}^{*-1} = (\mu d^2)^{-1} + (2\mathcal{J})^{-1}$ or $\mathcal{J}^* = 10/7\,\mathcal{J}$. In the limit of thermal equilibrium, the ℓ-distribution is:

$$P(\ell)d\ell = (2\pi\mathcal{J}^*T)^{-1/2} \exp -\left(\frac{\ell^2}{2\mathcal{J}^*T} - \frac{I\ell}{2\mathcal{J}T} + \frac{I^2\mathcal{J}^*}{8\mathcal{J}^2T}\right) \tag{3}$$

where T is the temperature. Introducing a 2IdI weight and the dimensionless variables $\varepsilon = E/T$, $\lambda = I/(\mathcal{J}T)^{1/2}$, we obtain the distribution function

$$P(\varepsilon,\lambda)d\varepsilon d\lambda \propto \frac{\lambda}{\sqrt{\varepsilon}} \exp -\left[\frac{7}{2}\varepsilon - \sqrt{\frac{5}{2}}\lambda\sqrt{\varepsilon} + \frac{5}{28}\lambda^2\right]d\varepsilon d\lambda \ . \tag{4}$$

The properties of this distribution function can be observed in the two-dimensional plot in Fig. 1 and can be summarized as follows.

<u>At constant ε</u> (a fixed cut in the exit channel kinetic energy), the most probable value of λ is:

$$\hat{\lambda} = \frac{7}{\sqrt{10}}\sqrt{\varepsilon}\left[1 + \sqrt{1 + \frac{4}{7\varepsilon}}\right] \tag{5}$$

to be compared with

$$\lambda = \frac{14}{\sqrt{10}}\sqrt{\varepsilon} \quad \text{from simple dynamics,}$$

while the width is given by

$$\sigma^2 = \frac{14}{5} \quad , \text{ independent of } \varepsilon! \tag{6}$$

Since $\mathcal{J}T$ is typically 100-200 $\hbar^2$, we have widths in the entrance channel angular momentum

$$17\hbar \leqslant \sigma \leqslant 24\hbar$$

$$40\hbar \leqslant \Gamma_{FWHM} \leqslant 56\hbar$$

for an infinitely sharp cut in the exit channel kinetic energy.

At constant λ (a fixed entrance-channel angular momentum), the average kinetic energy over the barrier is:

$$\bar{\varepsilon} = \frac{2}{7}\left(\frac{1}{2} + \frac{5}{28}\ \lambda^2\right) \tag{7}$$

while the width is:

$$\sigma^2 = \frac{4}{49}\left(\frac{1}{2} + \frac{5}{14}\ \lambda^2\right) \tag{8}$$

and

$$\frac{\sigma}{\varepsilon} = \frac{(1/2 + 5/14\lambda^2)^{1/2}}{1/2 + 5/28\ \lambda^2} \overset{\text{large } \lambda}{\simeq} 2\sqrt{\frac{14}{5}}\,\frac{1}{\lambda} \quad . \tag{9}$$

For an entrance channel angular momentum $I \simeq 240\ \hbar$, $\mathcal{J}T \simeq 144\ \hbar^2$, $T \simeq 3$ MeV, one obtains

$$\sigma = 10 \text{ MeV}$$

$$\Gamma_{FWHM} = 23.5 \text{ MeV},$$

while, for $I = 360\ \hbar$ (ℓrms for Ho + Ho at 8.5 MeV/A) one obtains:

$$\sigma = 15 \text{ MeV}$$

$$\Gamma_{FWHM} = 36 \text{ MeV}.$$

Examples of distributions in ε at fixed λ are shown in Fig. 2. The conclusion is that a sizeable mixing of entrance channel ℓ-waves is predicted for a fixed exit-channel kinetic energy by invoking just one thermally-excited wriggling mode.

We conclude this subject by calculating the kinetic energy distribution integrated over angular momentum from 0 to λ_{mx}. The integration yields:

$$P(\varepsilon) \propto \frac{1}{\sqrt{\varepsilon}}\left[e^{-\frac{7}{2}\varepsilon}\left\{1 - e^{-\frac{5}{28}\lambda_{mx}^2 + \sqrt{\frac{5}{2}}\lambda_{mx}\sqrt{\varepsilon}}\right\} + \sqrt{\frac{7\pi}{2}\varepsilon}\left\{\mathrm{erf}\left(\sqrt{\frac{5}{28}}\lambda_{mx} - \sqrt{\frac{7}{2}\varepsilon}\right) + \mathrm{erf}\left(\sqrt{\frac{7}{2}\varepsilon}\right)\right\}\right] . \qquad (10)$$

Plots of this distribution for different values of λ_{mx} are shown in Fig. 3. In order to appreciate better this result, we can calculate the corresponding distribution in the absence of fluctuations (T = 0) in the limit of rigid rotation:

The kinetic energy over the barrier is:

$$E = \frac{\ell^2}{2\mu d^2} = \frac{25}{49}\,\frac{I^2}{2\mu d^2}$$

which implies

$dE \propto dI^2$ for our model of two touching spheres.

But, from the entrance channel distribution, we have

$$P(\ell)d\ell = K2\ell d\ell = Kd\ell^2 = k'dI^2,$$

then

$$P(E)dE \propto dI^2 \propto dE \qquad 0 \leqslant I \leqslant I_{mx}$$

or, more precisely,

$$P(\varepsilon)d\varepsilon = \begin{cases} Kd\varepsilon & \varepsilon \leqslant \frac{5}{98}\lambda_{mx}^2 \\ 0 & \varepsilon > \frac{5}{98}\lambda_{mx}^2 \end{cases} .$$

In other words, we have a rectangular distribution. Examples of such distributions are also shown in Fig. 3.

3. SHAPE FLUCTUATIONS IN THE EXIT CHANNEL

It was realized, very early in the history of heavy ion reactions, that the observed sub-Coulomb emission of deep-inelastic fragments is due to their sizeable deformation at the scission point. The reasonably flat dependence of the total potential energy at scission as a function of deformation, together with the rather steep dependence of the two-fragment Coulomb interaction, leads to the possibility of fairly large shape fluctuations at scission with a resulting amplification of the fluctuations in the kinetic energy at infinity[6]. The role of deformation has also been considered by G. Wolschin and C. Riedel [7,8] in the context of a diffusion model and found to be important. The variation of both Coulomb energy and orbital energy with deformation suggests that shape fluctuation should lead to a smearing of a given entrance-channel ℓ-wave over a sizeable range of exit-channel kinetic energies.

For sake of simplicity, let us model the system at scission as composed of two equal and equally deformed spheroids in contact. The relevant total potential energy is

$$V_T = U_{LD}^{(1)}(\varepsilon) + U_{LD}^{(2)}(\varepsilon) + V_C^{*}(\varepsilon) + V_{rot}(I,\varepsilon) \tag{11}$$

where U_{LD}, V_C^{*}, V_{Rot} are the deformation dependent liquid drop energies [9,10], two fragment Coulomb interaction, and rotational energy, respectively. The common deformation of the fragments is ε and I is the angular momentum. In our model the potential energy has a minimum at a deformation ε_0 defined by

$$\frac{\partial V_T}{\partial \varepsilon} = 0 \quad .$$

The potential energy can be expanded quadratically about the minimum as

$$V_T \simeq V_0 + k(\varepsilon - \varepsilon_0)^2 \quad . \tag{12}$$

Similarly, the resulting kinetic energy at infinity is given by

$$E_{KE} = V_c^*(\varepsilon) + \frac{\ell(\varepsilon)^2}{2\mu d^2(\varepsilon)} \tag{13}$$

where V_c^* is the two-fragment Coulomb interaction, $\ell(\varepsilon)$ is the orbital angular momentum at scission determined from the rigid rotation condition, and d is the center-to-center distance. A linear expansion in ε about ε_0 leads to

$$E_{KE} \simeq E^0_{KE}(\varepsilon_0) + c(\varepsilon - \varepsilon_0) \quad .$$

In Fig. 4, the relevant potentials are plotted for the Fe + Fe system with 50 units of angular momentum. One sees that a small (energy-wise) fluctuation at scission, of the order of 1/2T in the thermal limit, leads to an amplified fluctuation in the final kinetic energy, so that

$$\sigma^2_{KE} = \frac{c^2}{2k}T = \frac{pT}{2} \tag{14}$$

where p is called the amplification parameter[4]. As can be seen in Fig. 4, this amplification is mostly due to the steepness of the Coulomb potential with deformation relative to the total potential energy. However, the contribution of the rotational energy term [see eq. (13)] to the width of the kinetic energy distribution is non-negligible. This distribution is, in fact, approximately a Gaussian

$$P(E_{KE}) \propto \exp - \frac{(E_{KE} - E^0_{KE})^2}{pT} \quad . \tag{15}$$

Certainly a great deal of the width in the final kinetic energy distribution arises from this effect. Even more interesting is the fact that the large spread in final kinetic energy is associated with a fixed total angular momentum. Of course, this feature has the effect of spreading any given ℓ-wave over a very broad range of kinetic energies, thus making the correlation between exit-channel kinetic energy and entrance-channel angular momentum very problematic.

Again, let us consider the system Fe + Fe. In Fig. 5 the kinetic energy distributions are shown for a set of ℓ values. While the centroid of the distribution moves towards higher values with increasing ℓ, the width also increases, leading to a dramatic overlap of distributions with widely different ℓ-values. Most interesting are the entrance-channel angular momentum distributions for a variety of exit-channel kinetic energies shown in Fig. 6. The distributions are so broad that at any kinetic energy the whole ℓ-wave spectrum is substantially sampled. The overall features of the distribution are shown by the two-dimensional plot in Fig. 7.

4. CONCLUSION

In conclusion, we have seen how the two processes described in sections 2 and 3 have the effect of spoiling the correlation between entrance-channel angular momentum and exit-channel kinetic energy. It is easy to think of other possible causes of similar nature. Still, in certain cases the picture may be made less dismal if the cross section is substantially spread-out in angle. Then we can hope for a correlation between exit-channel ℓ-value and angle. However, on one hand, this correlation is lost when strong focusing is present; and on the other, the correlation betwen exit-channel ℓ-value and entrance-channel angular momentum still remains hazy, as shown in section 2.

This work was supported by the Director, Office of Energy Research, Division of Nuclear Physics of the Office of High Energy and Nuclear Physics and by Nuclear Sciences of the Basic Energy Sciences Program of the U.S. Department of Energy under Contract W-7405-ENG-48.

References

1) Gross, D.H.E. and Kalinowski, H.: Phys. Lett. 48B, 302 (1974)

2) Randrup, J.: Nucl. Phys. A307, 319 (1978)

3) Davies, K.T.R., Maruhn-Rezwani, V., Koonin, S.E., and Negele, J.W.: Phys. Rev. Lett. 41, 632 (1978).

4) Gross, D.H.E., Nayak, R.C., and Satpathy, L.: Z. Physik A299, 63 (1981)

5) Moretto, L.G. and Schmitt, R.P.: Phys. Rev. C21, 204 (1980)

6) Moretto, L.G.: Nucl. Phys. A247, 211 (1975)

7) Wolschin, G.: Phys. Lett. 88B, 35 (1979)

8) Riedel, C. and Wolschin, G.: Z. Physik A294, 17 (1980)

9) Cohen, S. and Swiatecki, W.J.: Ann. Phys. 19, 67 (1962)

10) Nix, J.R. and Swiatecki, W.J.: Nucl. Phys. 71, 1 (1965)

Figure captions

Fig. 1. Two-dimensional plot of the distribution function given in eq. 4.

Fig. 2. Kinetic energy distributions for various values of the entrance-channel angular momentum.

Fig. 3. Angular-momentum-integrated kinetic energy distributions for different values of the maximum angular momentum. The box-like distributions defined by the vertical lines are obtained by eliminating fluctuations.

Fig. 4. Amplification of fluctuations at scission, illustrated for $^{56}Fe + ^{56}Fe$.

Fig. 5. Kinetic energy spectra for various values of the entrance-channel angular momentum for the system Fe + Fe.

Fig. 6. Entrance-channel angular momentum distributions for various values of exit-channel kinetic energies.

Fig. 7. Two-dimensional plot of the emission probability as a function of entrance-channel angular momentum and exit-channel kinetic energy.

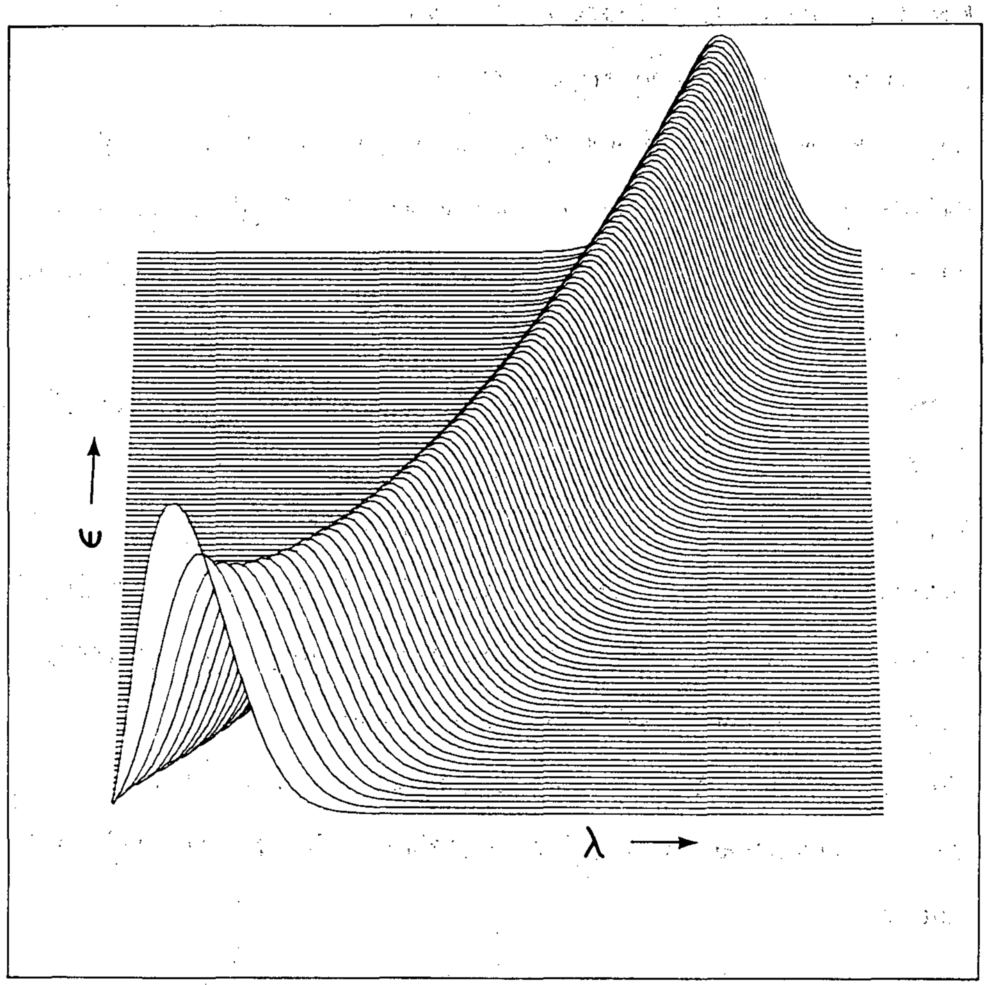

XBL 815-2268

Fig. 1

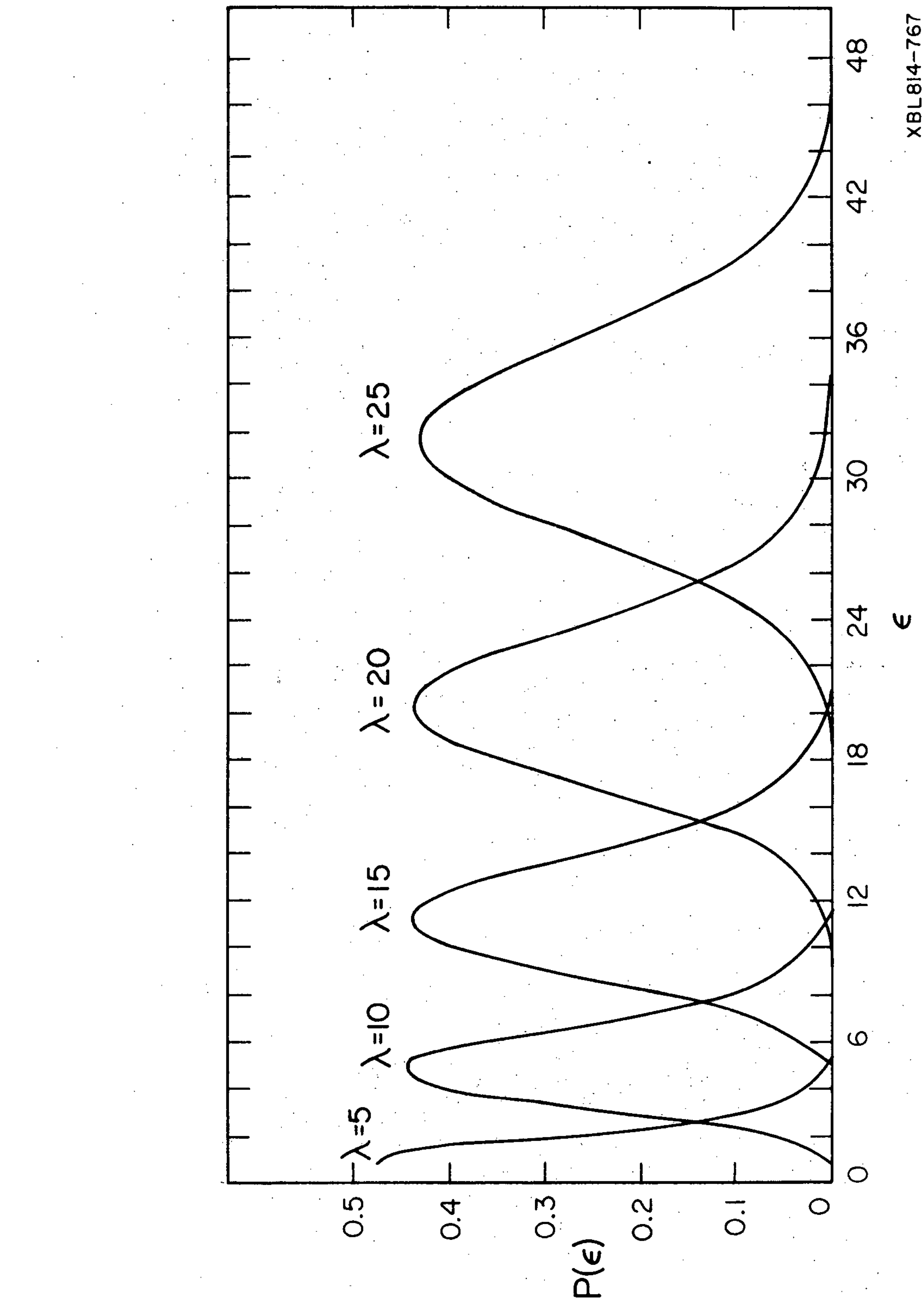
P(ε)
0.5
0.4
0.3
0.2
0.1
0
λ=5
λ=10
λ=15
λ=20
λ=25
0
6
12
18
24
30
36
42
48
ε
XBL814-767

Fig. 2

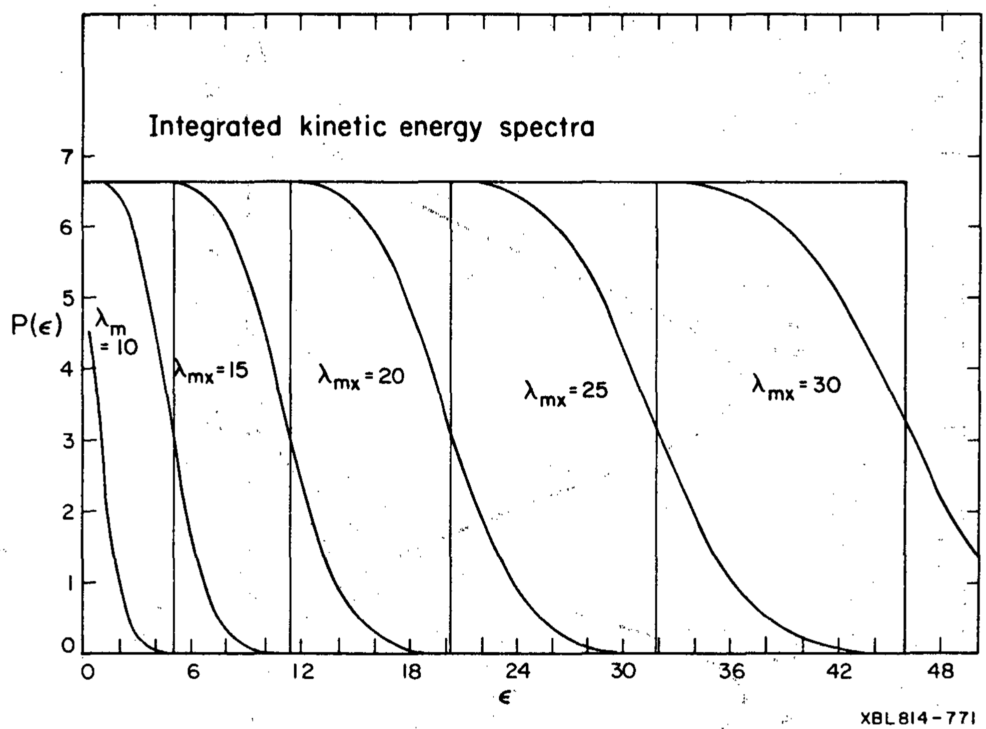
Integrated kinetic energy spectra
P(ε)
λm = 10
λmx=15
λmx=20
λmx=25
λmx=30
7
6
5
4
3
2
1
0
0
6
12
18
24
30
36
42
48
ε
XBL 814-771

Fig. 3

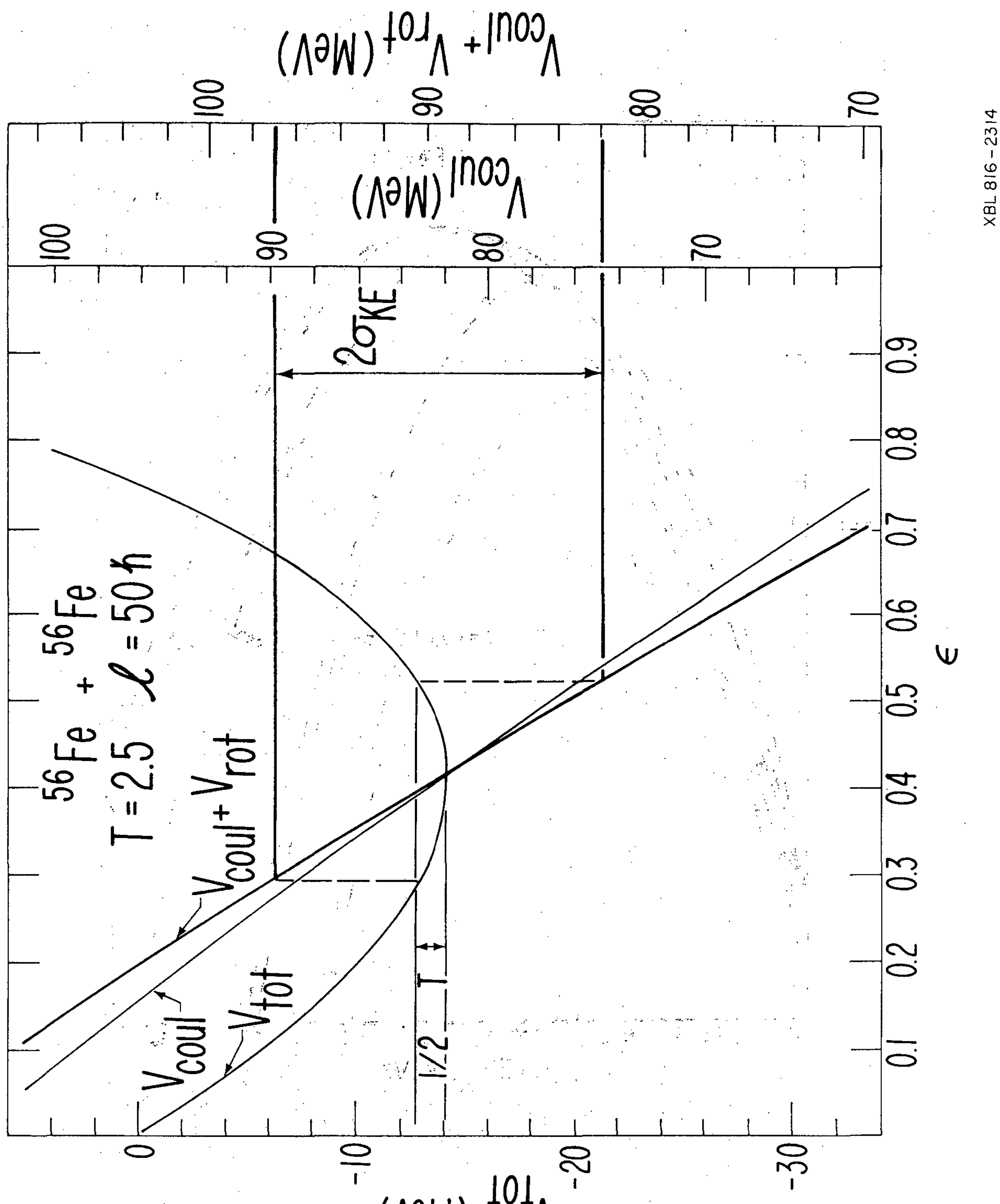

^{56}Fe + ^{56}Fe
T = 2.5 ℓ = 50ħ
V$_{coul}$+V$_{rot}$
V$_{coul}$
V$_{tot}$
2σ$_{KE}$
1/2 T
ε
0.1 0.2 0.3 0.4 0.5 0.6 0.7 0.8 0.9
0 -10 -20 -30
V$_{tot}$ (MeV)
100 90 80 70
V$_{coul}$ (MeV)
100 90 80 70
V$_{coul}$ + V$_{rot}$ (MeV)
XBL 816-2314

Fig. 4

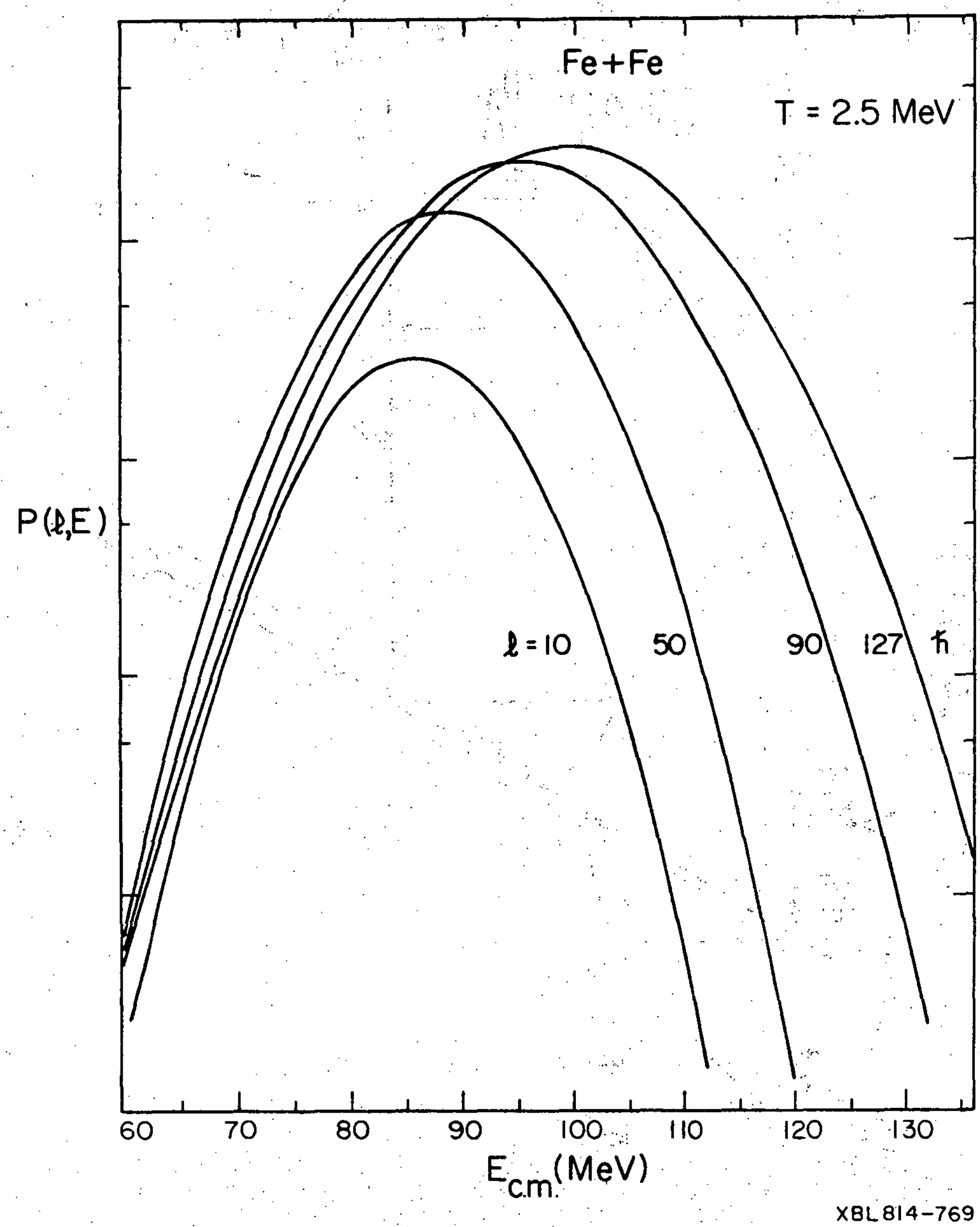
Fe+Fe
T = 2.5 MeV
P(ℓ,E)
ℓ=10
50
90
127
ħ
60
70
80
90
100
110
120
130
E_c.m.(MeV)
XBL 814-769

Fig. 5

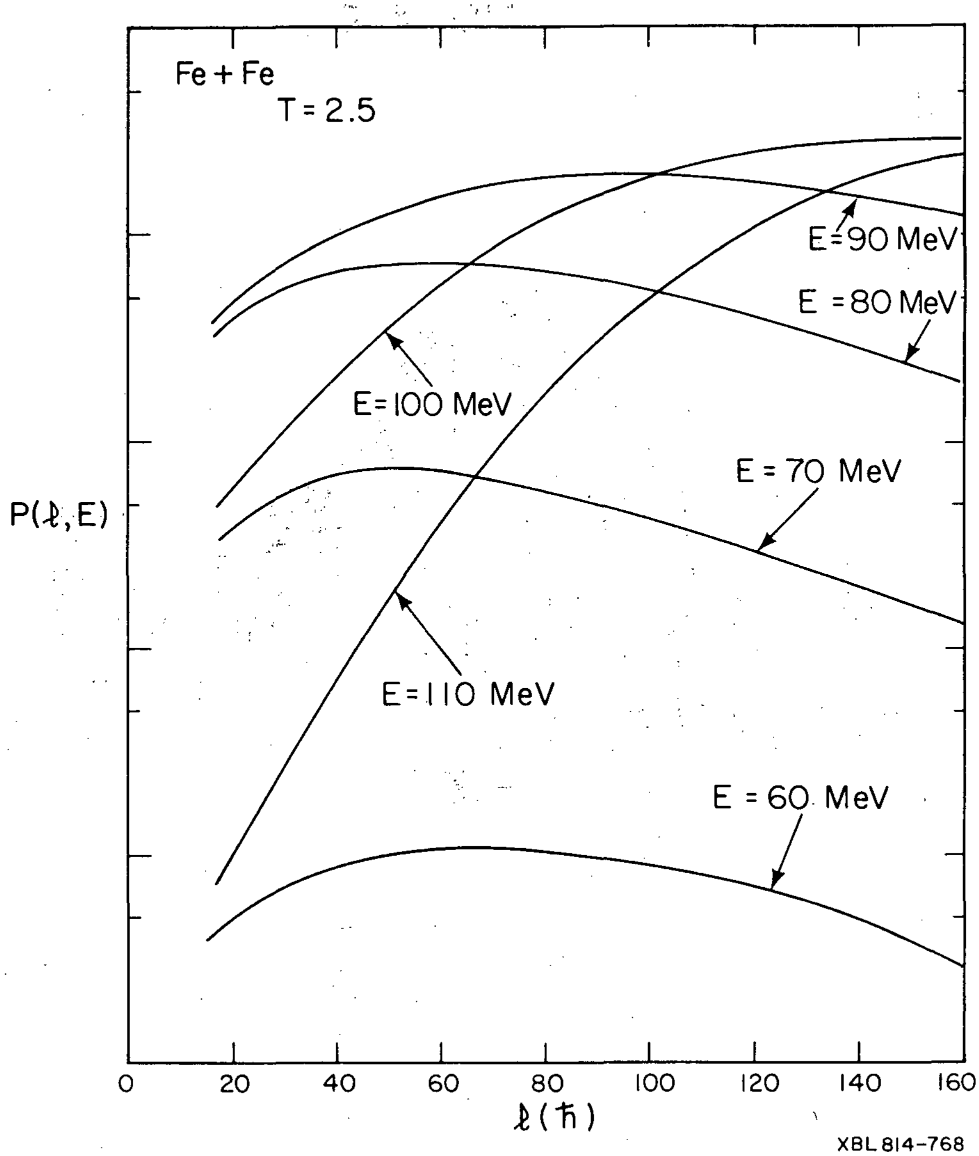

Fe + Fe
T = 2.5
E=90 MeV
E =80 MeV
E=100 MeV
E = 70 MeV
E=110 MeV
E = 60 MeV
P(ℓ,E)
0
20
40
60
80
100
120
140
160
ℓ(ħ)
XBL 814-768

Fig. 6

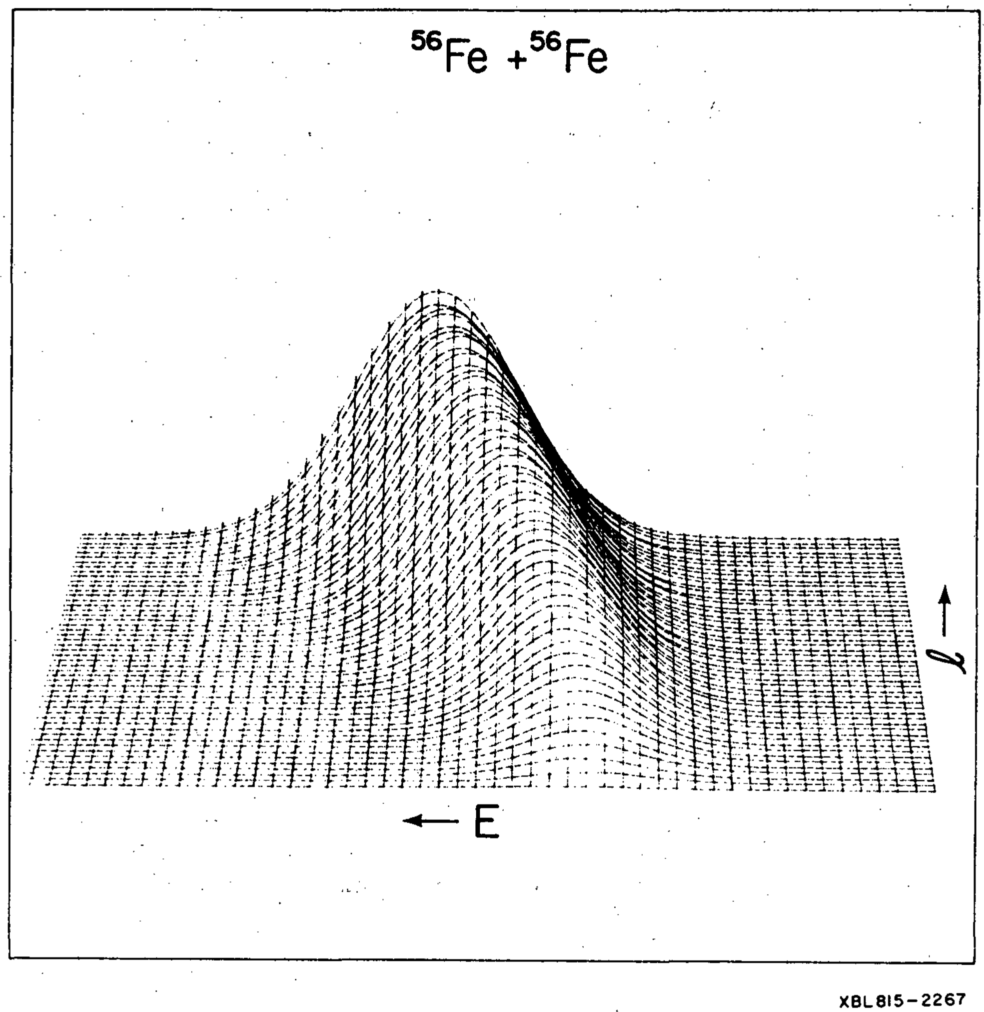

Fig. 7

TECHNICAL INFORMATION DEPARTMENT
LAWRENCE BERKELEY LABORATORY
UNIVERSITY OF CALIFORNIA
BERKELEY, CALIFORNIA 94720